УДК 539.3

FINITE ELEMENT FORMULATION OF STRAIGHT COMPOSITE BEAMS UNDERGOING FINITE ROTATIONS

G.M. Kulikov, S.V. Plotnikova

Department of Applied Mathematics and Mechanics, TSTU

Key Words and Phrases: finite rotations; Timoshenko beam theory; large rigid body motions.

Abstract: A simple and efficient mixed finite element model is developed for the analysis of straight multilayered composite Timoshenko beams undergoing finite rotations by using the total Lagrangian formulation in conjunction with the Newton-Raphson method. The effects of the transverse shear and transverse normal strains, and laminated material response are included. The precise representation of arbitrarily large rigid body motions in the displacement patterns of refined non-linear Timoshenko beam elements is considered. The fundamental unknowns consist of four displacements and five strains of the face lines of the beam, and five stress resultants. The element characteristics arrays are obtained by using the Hu-Washizu mixed variational principle. To demonstrate the efficiency and accuracy of this formulation and to compare its performance with other non-linear finite element models reported in the literature, numerical studies are presented.

1 Introduction

One of the main requirements of a finite element that is intended for the general non-linear analysis is that it must lead to strain-free modes for large rigid body motions. The adequate representation of large rigid body motions is a necessary condition if a non-linear element is to have the good accuracy and convergence properties. Therefore, when an inconsistent non-linear theory is used to construct any finite element, erroneous straining modes under arbitrarily large rigid body motions may be appeared. This problem has been studied for the geometrically linear Kirchhoff-Love shell theory in [1, 2] and Timoshenko-Mindlin-type (**TMT**) shell theory in [3, 4].

Herein, the more general study on the basis of the refined large deformation Timoshenko beam theory taking into account the transverse normal deformation response is considered. As unknown functions four displacements of the face lines of the beam are chosen [5-7]. Such choice of the displacements gives the possibility to deduce the non-linear strain-displacement equations, which are completely free for large rigid body motions.

Using the traditional non-linear TMT theory in a finite element formulation for beams, plates and shells is well established and has been shown to give acceptable results [8-16]. This theory has the advantage that displacement and rotation trial functions may be used and these functions need only to be C° continuous. The developed refined non-linear Timoshenko beam theory has the essential advantage, since only independent trial functions of displacements of the face lines may be used [3, 4]. Our theory is free of the assumptions of small displacements, small rotations, small strains and small loading steps.

The finite element formulation is based on a simple and efficient approximation of shells via quadrilateral four-node elements developed by Hughes and Tezduyar [17]. The fundamental unknowns consist of four displacements and five strains of the face lines of a beam and five stress resultants. The simplest admissible approximations of the one-dimensional fields are used, namely, linear approximations of the displacements and transverse normal strain, and constant approximations of other strains. The element characteristic arrays are obtained by using the Hu-Washizu mixed variational principle in conjunction with the total Lagrangian formulation and Newton-Raphson method.

The numerical results are presented to demonstrate the efficiency and high accuracy of the developed finite element model and to compare its performance with other approaches reported in literature. For this purpose three tests are employed.

2 Strain-displacement equations

Let us consider a straight beam of the uniform thickness h. The beam may be defined as a 2-D body bounded by two bounding lines S^- and S^+, located at the distances δ^- and δ^+ measured with respect to the reference line S^r, and the edge boundary lines Ω^- and Ω^+ that are perpendicular to the reference line. Let the coordinates x_1 and x_3 denote the direction of the reference line S^r and the transverse direction. The initial configuration of a beam segment at time t_0 is shown in Fig. 1, *a* while Fig. 1, *b* illustrates the current configuration at time t.

The components of the Green-Lagrange strain tensor for large displacements and strains can be written in a vector form as

$$\varepsilon_{ii}^{e} = \frac{\partial \mathbf{u}}{\partial x_i}\left(\mathbf{e}_i + \frac{1}{2}\frac{\partial \mathbf{u}}{\partial x_i}\right) \qquad (i = 1, 3),$$
$$2\varepsilon_{13}^{e} = \frac{\partial \mathbf{u}}{\partial x_1}\left(\mathbf{e}_3 + \frac{1}{2}\frac{\partial \mathbf{u}}{\partial x_3}\right) + \frac{\partial \mathbf{u}}{\partial x_3}\left(\mathbf{e}_1 + \frac{1}{2}\frac{\partial \mathbf{u}}{\partial x_1}\right), \qquad (1)$$

where $\mathbf{u} = u_1\mathbf{e}_1 + u_3\mathbf{e}_3$ is the displacement vector; $u_i(x_1, x_3)$ are the components of this vector, which are always measured in accordance with the total Lagrangian formulation from the initial configuration to the current configuration directly; $\mathbf{e}_1$ and $\mathbf{e}_3$ are the unit base vectors of the Cartesian coordinate frame (Fig. 1).

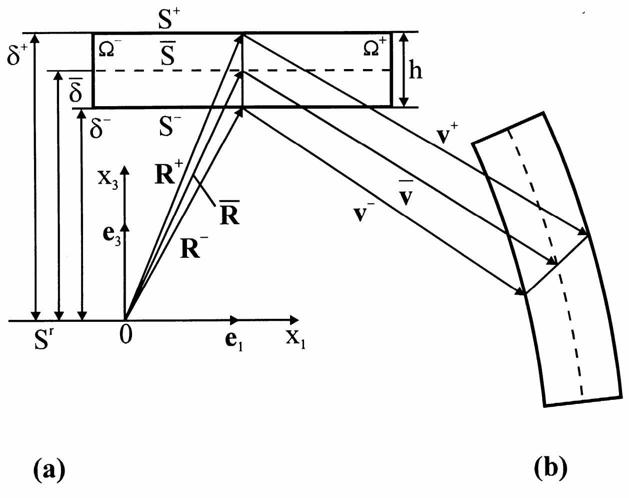

Fig. 1 Beam element: (a) initial configuration and (b) current configuration

The refined large deformation Timoshenko beam theory is based on the linear approximation of the displacements in the thickness direction [5-7]:

$$\mathbf{u} = N^-(x_3)\mathbf{v}^- + N^+(x_3)\mathbf{v}^+,$$
$$N^-(x_3) = (\delta^+ - x_3)/h, \qquad N^+(x_3) = (x_3 - \delta^-)/h, \tag{2}$$

where $\mathbf{v}^{\pm} = v_1^{\pm}\mathbf{e}_1 + v_3^{\pm}\mathbf{e}_3$ are the displacement vectors of the face lines $S^{\pm}$; $v_i^{\pm}(x_1)$ are the displacements of the face lines $(i = 1, 3)$; $N^{\pm}(x_3)$ are the linear shape functions. The linear approximation (2) may be considered as a refined Timoshenko kinematic hypothesis [18, 19]. The advantage of the proposed approach is apparent, since with the help of the displacements $v_i^{\pm}$ the kinematic boundary conditions on the face lines of the beam can be formulated. Moreover, this simplifies a formulation of new finite element beam-shell models [3, 4] and provides a convenient way to express the non-linear strain-displacement relationships in terms of face line-surface strains [5, 7].

Substituting the displacements (2) into the strain-displacement equations (1), one can obtain the strain-displacement equations of the refined large deformation Timoshenko theory of moderately thick beams:

$$\varepsilon_{11}^a = \left[N^-(x_3)\mathbf{v}_{,1}^- + N^+(x_3)\mathbf{v}_{,1}^+\right]\mathbf{e}_1 + \frac{1}{2}\left[N^-(x_3)\mathbf{v}_{,1}^- + N^+(x_3)\mathbf{v}_{,1}^+\right]^2, \tag{3}$$

$$2\varepsilon_{13}^a = \boldsymbol{\beta}\mathbf{e}_1 + \mathbf{v}_{,1}(\mathbf{e}_3 + \boldsymbol{\beta}) + (x_3 - \bar{\delta})\varepsilon_{33,1}^a, \qquad \varepsilon_{33}^a = \boldsymbol{\beta}\left(\mathbf{e}_3 + \frac{1}{2}\boldsymbol{\beta}\right),$$

$$\boldsymbol{\beta} = \frac{1}{h}(\mathbf{v}^+ - \mathbf{v}^-), \qquad \mathbf{v} = \frac{1}{2}(\mathbf{v}^- + \mathbf{v}^+), \tag{4}$$

where $\bar{\delta} = (\delta^- + \delta^+)/2$ is the distance from the reference line to the middle line $\bar{S}$ of the beam. Here and in the following developments the abbreviation $(\ )_{,1}$ implies the ordinary derivative with respect to the coordinate x_1.

The strain-displacement equations (3) and (4) are very attractive because they are completely free for arbitrarily large rigid body motions. It will be shown in the next section. Note also that the longitudinal strain ε_{11}^a is distributed over the beam thickness according to the quadratic law. Taking into account that a beam has a moderate thickness, this complication of the Timoshenko beam theory would be unreasonable because of the minor significance of the quadratic term in most problems.

Therefore, more convenient strain-displacement equations of the refined large deformation Timoshenko beam theory can be written as

$$\varepsilon_{11}^b = N^-(x_3)\mathbf{v}_{,1}^-\left(\mathbf{e}_1 + \frac{1}{2}\mathbf{v}_{,1}^-\right) + N^+(x_3)\mathbf{v}_{,1}^+\left(\mathbf{e}_1 + \frac{1}{2}\mathbf{v}_{,1}^+\right), \tag{5}$$

$$2\varepsilon_{13}^b = \boldsymbol{\beta}\mathbf{e}_1 + \mathbf{v}_{,1}(\mathbf{e}_3 + \boldsymbol{\beta}) + (x_3 - \bar{\delta})\varepsilon_{33,1}^b, \qquad \varepsilon_{33}^b = \boldsymbol{\beta}\left(\mathbf{e}_3 + \frac{1}{2}\boldsymbol{\beta}\right).$$

These strain-displacement equations are also completely free for large rigid body motions.

It is important to note that deduced strain-displacement equations (3)-(5) satisfy the following coupling conditions:

$$\varepsilon_{11}^a(\delta^{\pm}) = \varepsilon_{11}^b(\delta^{\pm}) = E_{11}^{\pm}, \tag{6}$$

where $E_{11}^{\pm}$ are the longitudinal strains of the face lines $S^{\pm}$ defined as

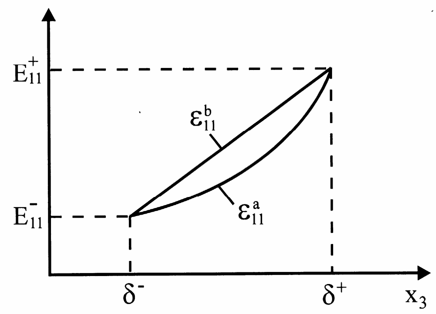

Fig. 2 Distribution of longitudinal strain over beam thickness

$$E_{11}^{\pm} = \mathbf{v}_{,1}^{\pm}\left(\mathbf{e}_1 + \frac{1}{2}\mathbf{v}_{,1}^{\pm}\right). \qquad (7)$$

This statement is illustrated in Fig. 2.

Finally, consider a limit case when the transverse displacement u_3 is independent on the coordinate x_3, i.e., $v_3^{-} = v_3^{+} = v_3$. Such case corresponds to the refined Timoshenko beam theory without thickness change. In a result we have the following strain-displacement equations:

$$\begin{gathered}\varepsilon_{11}^{c} = N^{-}(x_3)\mathbf{v}_{,1}^{-}\left(\mathbf{e}_1 + \frac{1}{2}\mathbf{v}_{,1}^{-}\right) + N^{+}(x_3)\mathbf{v}_{,1}^{+}\left(\mathbf{e}_1 + \frac{1}{2}\mathbf{v}_{,1}^{+}\right),\\ 2\varepsilon_{13}^{c} = \boldsymbol{\beta}\mathbf{e}_1 + \mathbf{v}_{,1}(\mathbf{e}_3 + \boldsymbol{\beta}), \qquad \varepsilon_{33}^{c} = 0,\end{gathered} \qquad (8)$$

where $\mathbf{v}^{\pm} = v_1^{\pm}\mathbf{e}_1 + v_3\mathbf{e}_3$ are the displacement vectors of the face lines. As we shall see in the next section, the strain-displacement equations (8) and (4) can never be free for the large rigid body motions.

3 Large rigid body motions

An arbitrarily large rigid body motion can be defined as

$$\mathbf{u}^{R} = \boldsymbol{\Delta} + (\mathbf{A} - \mathbf{E})\mathbf{R}, \qquad (9)$$

where $\mathbf{R} = x_1\mathbf{e}_1 + x_3\mathbf{e}_3$ is the position vector of any point of the beam; $\boldsymbol{\Delta} = \Delta_1\mathbf{e}_1 + \Delta_3\mathbf{e}_3$ is the constant displacement (translation) vector; **E** is the identity matrix; **A** is the orthogonal rotation matrix defined as

$$\mathbf{A} = \begin{bmatrix} \cos\varphi & \sin\varphi \\ -\sin\varphi & \cos\varphi \end{bmatrix}, \qquad (10)$$

where φ is the rotation angle of a beam around the point O (Fig. 1).

In particular, rigid body motions of the face lines are

$$\mathbf{v}^{\pm R} = \boldsymbol{\Delta} + (\mathbf{A} - \mathbf{E})\mathbf{R}^{\pm}, \qquad (11)$$

where $\mathbf{R}^{\pm} = x_1\mathbf{e}_1 + \delta^{\pm}\mathbf{e}_3$ are the position vectors of points of the top and bottom lines $S^{\pm}$ (Fig. 1).

The derivatives of the translation vector and the position vectors of the face lines with respect to the coordinate x_1 can be written as

$$\boldsymbol{\Delta}_{,1} = \mathbf{0}, \qquad \mathbf{R}_{,1}^{\pm} = \mathbf{e}_1. \qquad (12)$$

Taking into account formulas (10)-(12), one can obtain the following expression for the derivatives:

$$\mathbf{v}_{,1}^{\pm R} = \mathbf{A}\mathbf{e}_1 - \mathbf{e}_1. \qquad (13)$$

It can be verified by using formulas (11) and (13) that strains from relationships (3)-(5) are all zero in a general large rigid body motion, i.e.,

$$\varepsilon_{ii}^{aR} = \frac{1}{2}\left[(\mathbf{Ae}_i)(\mathbf{Ae}_i) - \mathbf{e}_i\mathbf{e}_i\right] = 0 \qquad (i = 1,3),$$
$$2\varepsilon_{13}^{aR} = (\mathbf{Ae}_1)(\mathbf{Ae}_3) - \mathbf{e}_1\mathbf{e}_3 + \left(x_3 - \bar{\delta}\right)\varepsilon_{33,1}^{aR} = 0. \qquad (14)$$

This conclusion is true since an orthogonal transformation retains the scalar product of the vectors. To write the remaining equations, we should replace in Eq. (14) the superscript a by b.

So, our refined large deformation Timoshenko beam theory is completely strain-free for all large rigid body motions. It should be noted that using a similar technique the more general large deformation layer-wise Timoshenko beam theory can be developed. This theory is under development and will be published in the next paper.

To investigate the possibility of the simplified strain-displacement equations (8) and (4) to represent adequately the large rigid body motions, we consider an equation that simply follows from Eqs. (10) and (11):

$$v_3^{\pm R} = \Delta_3 - x_1 \sin\varphi + \delta^{\pm}(\cos\varphi - 1), \qquad (15)$$

It can be seen from Eq. (15) that $v_3^{-R} \neq v_3^{+R}$. But it is impossible since in this Timoshenko beam model the transverse displacement is independent on the coordinate x_3. So, the large deformation Timoshenko beam theory neglecting the transverse normal strain can never be strain-free for arbitrarily large rigid body motions. Further, we shall see that it is a serious deficiency of the classical Timoshenko theory of beams undergoing large rotations.

4 Hu-Washizu functional for multilayered composite beam

Let us consider a beam built up in the general case by the arbitrary superposition across the thickness of N layers of uniform thickness h_k. The *k*th layer may be defined as a 2-D body bounded by two lines S_{k-1} and S_k, located at the distances δ_{k-1} and δ_k measured with respect to the reference line S^r, and the edge boundary lines $\Omega_k^{\pm}$ that are perpendicular to the reference line (Fig. 3). Let the reference line be referred to the coordinate x_1. The x_3 axis is oriented to the normal direction.

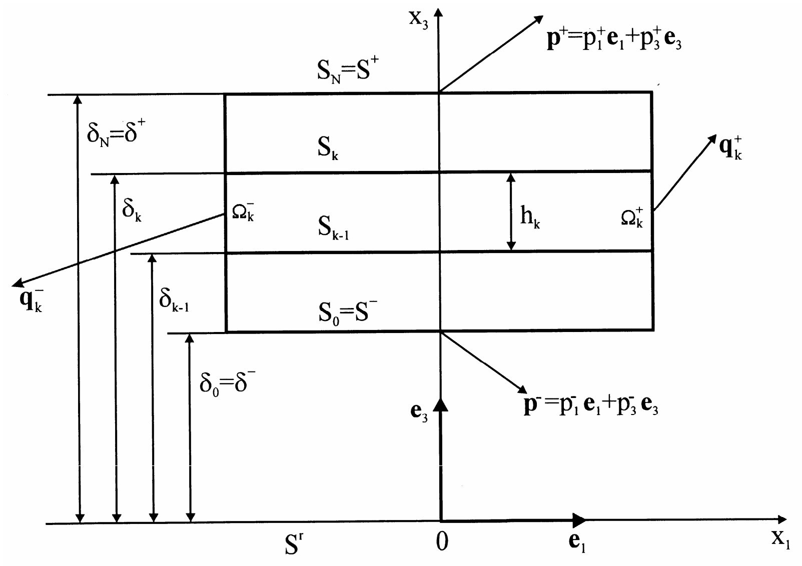

Fig. 3 Multilayered beam

The constituent layers of the beam are supposed to be rigidly joined, so that no slip on contact lines and no separation of layers can occur. The material of each constituent layer is assumed to be linearly elastic and orthotropic. Let p_i^- and p_i^+ be the intensities of the external loading acting on the bottom line $S^- = S_0$ and top line $S^+ = S_N$ in the x_i coordinate directions, respectively; $\mathbf{q}_k^{\pm} = q_1^{(k)\pm}\mathbf{e}_1 + q_3^{(k)\pm}\mathbf{e}_3$ are the external loading vectors acting on the edge boundary lines $\Omega_k^{\pm}$. Here and in the following developments the index k identifies the belonging of any quantity to the *k*th layer $\left(k = \overline{1, N}\right)$, and index i takes the values 1 and 3.

The refined large deformation Timoshenko theory of multilayered composite beams is based on the linear approximation of the displacement vector in the thickness direction (2), where we should set $\delta^- = \delta_0$ and $\delta^+ = \delta_N$. Substituting the displacements (2) and strains rewritten in the more convenient form

$$\varepsilon_{1i} = N^-(x_3)E_{1i}^- + N^+(x_3)E_{1i}^+, \qquad \varepsilon_{33} = E_{33} \tag{16}$$

into the Hu-Washizu functional [20], and accounting for the strain-displacement relationships (5), one can obtain

$$J = \int_{S^r} \Big\{ \Pi\left(E_{1i}^{\pm}, E_{33}\right) - \sum_i \Big[H_{1i}^-\left(E_{1i}^- - e_{1i}^- - \eta_{1i}^-\right) + $$
$$+ H_{1i}^+\left(E_{1i}^+ - e_{1i}^+ - \eta_{1i}^+\right)\Big] - H_{33}\left(E_{33} - e_{33} - \eta_{33}\right)\Big\} dx_1 + \int_{S^-} \sum_i p_i^- v_i^- dx_1 - \int_{S^+} \sum_i p_i^+ v_i^+ dx_1 - \tag{17}$$
$$- \sum_i \left(\tilde{H}_{1i}^- v_i^- + \tilde{H}_{1i}^+ v_i^+ \right) \Bigg|_{x_1^-}^{x_1^+},$$

where

$$e_{11}^{\pm} = \lambda_1^{\pm}, \qquad e_{13}^{\pm} = \beta_1 - \theta_1^{\pm}, \qquad e_{33} = \beta_3, \tag{18}$$
$$\eta_{11}^{\pm} = \frac{1}{2}\left(\lambda_1^{\pm}\right)^2 + \frac{1}{2}\left(\theta_1^{\pm}\right)^2, \qquad \eta_{13}^{\pm} = \beta_1\lambda_1^{\pm} - \beta_3\theta_1^{\pm}, \qquad \eta_{33} = \frac{1}{2}\beta_1^2 + \frac{1}{2}\beta_3^2,$$
$$\beta_i = \frac{1}{h}\left(v_i^+ - v_i^-\right), \qquad \lambda_1^{\pm} = v_{1,1}^{\pm}, \qquad \theta_1^{\pm} = -v_{3,1}^{\pm},$$

where Π is the strain energy density; $E_{1i}^{\pm}$ are the tangential normal and transverse shear strains of the face lines $S^{\pm}$; E_{33} is the transverse normal strain of the middle line; and $H_{1i}^{\pm}$ are the generalized stress resultants; H_{33} is the classical stress resultant, which are defined as

$$\Pi = \frac{1}{2}\sum_i \left[D_{1i1i}^{00}\left(E_{1i}^-\right)^2 + 2D_{1i1i}^{01}E_{1i}^-E_{1i}^+ + D_{1i1i}^{11}\left(E_{1i}^+\right)^2 \right] + $$
$$+ D_{1133}^{0}E_{11}^-E_{33} + D_{1133}^{1}E_{11}^+E_{33} + \frac{1}{2}D_{3333}E_{33}^2, \tag{19}$$

$$D_{1i1i}^{pq} = \sum_k \int_{\delta_{k-1}}^{\delta_k} C_{1i1i}^{(k)}\left[N^-(x_3)\right]^{2-p-q}\left[N^+(x_3)\right]^{p+q} dx_3 \qquad (p, q = 0, 1),$$

$$D^{p}_{1133} = \sum_k \int_{\delta_{k-1}}^{\delta_k} C^{(k)}_{1133} \left[N^{-}(x_3)\right]^{1-p} \left[N^{+}(x_3)\right]^{p} dx_3 \qquad (p = 0, 1),$$

$$D_{3333} = \sum_k \int_{\delta_{k-1}}^{\delta_k} C^{(k)}_{3333} dx_3,$$

and

$$H^{\pm}_{1i} = \sum_k \int_{\delta_{k-1}}^{\delta_k} S^{(k)}_{1i} N^{\pm}(x_3) dx_3, \qquad H_{33} = \sum_k \int_{\delta_{k-1}}^{\delta_k} S^{(k)}_{33} dx_3, \tag{20}$$

$$\tilde{H}^{\pm}_{1i} = \sum_k \int_{\delta_{k-1}}^{\delta_k} q^{(k)}_i N^{\pm}(x_3) dx_3.$$

In formulas (20) $S^{(k)}_{1i}$ and $S^{(k)}_{33}$ denote the components of the second Piola-Kirchhoff stress tensor of the *k*th layer that can be found by using the complete 2-D stress-strain relationships as

$$\begin{bmatrix} S^{(k)}_{11} \\ S^{(k)}_{33} \\ S^{(k)}_{13} \end{bmatrix} = \begin{bmatrix} C^{(k)}_{1111} & C^{(k)}_{1133} & 0 \\ C^{(k)}_{3311} & C^{(k)}_{3333} & 0 \\ 0 & 0 & C^{(k)}_{1313} \end{bmatrix} \begin{bmatrix} \varepsilon_{11} \\ \varepsilon_{33} \\ \varepsilon_{13} \end{bmatrix}, \tag{21}$$

where $\varepsilon_{ii} = \varepsilon^{b}_{ii}$ and $\varepsilon_{13} = 2\varepsilon^{b}_{13}$ are strains defined by Eqs. (5) and (16).

In a case of the multilayered isotropic beam we have the following expressions for the stiffness coefficients:

$$C^{(k)}_{1111} = C^{(k)}_{3333} = \frac{E_k}{1 - \nu_k^2}, \tag{22}$$

$$C^{(k)}_{1133} = C^{(k)}_{3311} = \frac{\nu_k E_k}{1 - \nu_k^2}, \qquad C^{(k)}_{1313} = \frac{E_k}{2(1 + \nu_k)},$$

where E_k and ν_k are Young's modulus and Poisson's ratio of the *k*th layer. As typically for the 2-D beam formulation, the rectangular cross-section area A and the inertia moment I are defined as

$$A = bh, \qquad I = bh^3 / 12, \qquad b = 1. \tag{23}$$

These formulas will be used in section 6.

5 Finite element formulation

The Hu-Washizu functional (17) for the element can be rewritten in a matrix form

$$J^{e\ell} = \int_{-1}^{1} \left[\frac{1}{2} \mathbf{E}^{T} \mathbf{D} \mathbf{E} - \left(\mathbf{E}^{T} - \mathbf{e}^{T} - \boldsymbol{\eta}^{T} \right) \mathbf{H} - \mathbf{v}^{T} \mathbf{P} \right] d\xi_1 - \mathbf{v}^{T} \tilde{\mathbf{H}} \Big|_{-1}^{1}, \tag{24}$$

where ξ_1 is the local coordinate of the element; $\mathbf{v} = \left[v^{-}_1 \; v^{+}_1 \; v^{-}_3 \; v^{+}_3\right]^{T}$ is the displacement vector; $\mathbf{E} = \left[E^{-}_{11} \; E^{+}_{11} \; E^{-}_{13} \; E^{+}_{13} \; E_{33}\right]^{T}$ is the strain vector; $\mathbf{e} = \left[e^{-}_{11} \; e^{+}_{11} \; e^{-}_{13} \; e^{+}_{13} \; e_{33}\right]^{T}$ and $\boldsymbol{\eta} = \left[\eta^{-}_{11} \; \eta^{+}_{11} \; \eta^{-}_{13} \; \eta^{+}_{13} \; \eta_{33}\right]^{T}$ are the linear and non-linear parts of the strain-displacement transformation vector; $\mathbf{H} = \left[H_{11}^{-}\ H_{11}^{+}\ H_{13}^{-}\ H_{13}^{+}\ H_{33} \right]^{T}$ is the stress resultant vector; $\mathbf{\bar{H}} = \left[\bar{H}_{11}^{-}\ \bar{H}_{11}^{+}\ \bar{H}_{13}^{-}\ \bar{H}_{13}^{+} \right]^{T}$ is the loading resultant vector acting on the edges of the element; $\mathbf{P} = \left[-p_1^{-}\ \ p_1^{+} - p_3^{-}\ \ p_3^{+} \right]^{T}$ is the surface traction vector; **D** is the constitutive stiffness matrix of order 5×5, which components are defined by Eq. (19).

For the simplest two-node beam element the displacement field is approximated according to the standard C° interpolation

$$\mathbf{v} = N_1(\xi_1)\mathbf{v}_1 + N_2(\xi_1)\mathbf{v}_2, \tag{25}$$

where $N_j(\xi_1)$ are the linear shape functions of the element; $\mathbf{v}_j = \left[v_{1j}^{-}\ v_{1j}^{+}\ v_{3j}^{-}\ v_{3j}^{+} \right]^{T}$ are the displacement vectors of the element nodes; the index j denotes a number of nodes and equals 1 and 2. The load vector is also assumed to vary linearly inside the element.

In accordance with the assumed strain concept, developed by Hughes and Tezduyar [17], the following strain interpolations are adopted:

$$\mathbf{E} = \overset{\circ}{\mathbf{E}} + \xi_1 \mathbf{Q} \hat{\mathbf{E}}, \tag{26}$$

$$\overset{\circ}{\mathbf{E}} = \left[\overset{\circ}{E}{}_{11}^{-}\ \overset{\circ}{E}{}_{11}^{+}\ \overset{\circ}{E}{}_{13}^{-}\ \overset{\circ}{E}{}_{13}^{+}\ \overset{\circ}{E}{}_{33} \right]^{T}, \qquad \hat{\mathbf{E}} = \left[\hat{E}_{33} \right],$$

$$\mathbf{Q} = \left[0\ 0\ 0\ 0\ 1 \right]^{T}, \tag{27}$$

where $\overset{\circ}{\mathbf{E}}$ is the vector of homogeneous states of strains; $\hat{\mathbf{E}}$ is the 1×1 matrix of the higher approximation modes of strains. Note that a vector **Q** in Eq. (27) is introduced for convenience and simplifies matrix routines.

The interpolations of the stress resultants follow the forms of the conjugate strains

$$\mathbf{H} = \overset{\circ}{\mathbf{H}} + \xi_1 \mathbf{Q} \hat{\mathbf{H}}, \tag{28}$$

$$\overset{\circ}{\mathbf{H}} = \left[\overset{\circ}{H}{}_{11}^{-}\ \overset{\circ}{H}{}_{11}^{+}\ \overset{\circ}{H}{}_{13}^{-}\ \overset{\circ}{H}{}_{13}^{+}\ \overset{\circ}{H}{}_{33} \right]^{T}, \qquad \hat{\mathbf{H}} = \left[\hat{H}_{33} \right].$$

Accounting for the strain-displacement relationships (18) and substituting the Eqs. (25)-(28) into the functional (24), one can obtain using the standard variational procedure the governing equations of the present finite element formulation

$$\overset{\circ}{\mathbf{E}} = \left(\overset{\circ}{\mathbf{B}} + \overset{\circ}{\mathbf{R}}\mathbf{u} \right)\mathbf{u}, \qquad \hat{\mathbf{E}} = \mathbf{Q}^{T}\left(\hat{\mathbf{B}} + \hat{\mathbf{R}}\mathbf{u} \right)\mathbf{u}, \tag{29a}$$

$$\overset{\circ}{\mathbf{H}} = \mathbf{D}\overset{\circ}{\mathbf{E}}, \qquad \hat{\mathbf{H}} = \mathbf{Q}^{T}\mathbf{D}\mathbf{Q}\hat{\mathbf{E}}, \tag{29b}$$

$$\left(\overset{\circ}{\mathbf{B}} + 2\overset{\circ}{\mathbf{R}}\mathbf{u} \right)^{T} \overset{\circ}{\mathbf{H}} + \frac{1}{3}\left(\hat{\mathbf{B}} + 2\hat{\mathbf{R}}\mathbf{u} \right)^{T} \mathbf{Q}\hat{\mathbf{H}} = \mathfrak{I}, \tag{29c}$$

where $\mathbf{u} = \left[\mathbf{v}_1^{T}\ \ \mathbf{v}_2^{T} \right]^{T}$ is the displacement vector at nodal points of the element; $\mathfrak{I}$ is the force vector; $\overset{\circ}{\mathbf{B}}$ and $\hat{\mathbf{B}}$ are the matrices of order 5×8, corresponding to the linear strain-displacement transformation; $\overset{\circ}{\mathbf{R}}$ and $\hat{\mathbf{R}}$ are the 3-D arrays of order $5 \times 8 \times 8$, corresponding to the non-linear strain-displacement transformation. It is apparent that in

Eqs. (29a) and (29c) $\overset{\circ}{\mathbf{R}}\mathbf{u}$ and $\overset{\wedge}{\mathbf{R}}\mathbf{u}$ imply matrices of order 5×8, and the following rule is used in calculations:

$$\left(\overset{\circ}{R}u\right)_{\ell m} = \overset{\circ}{R}_{\ell mn}u_n, \qquad \left(\hat{R}u\right)_{\ell m} = \hat{R}_{\ell mn}u_n \qquad \left(\ell = \overline{1,5};\ \ m,n = \overline{1,8}\right),$$

where the summation on the repeated index n is implied.

It is important to note that due to an approach developed in Ref. [3] the following coupling equation can be deduced:

$$h\hat{E}_{33} = \overset{\circ}{E}{}^{+}_{13} - \overset{\circ}{E}{}^{-}_{13}. \tag{30}$$

Besides, all matrix calculations are evaluated by using the full exact integration.

Up to this moment, no incremental arguments are needed in the total Lagrangian formulation. The incremental displacements, strains and stress resultants are needed in solving the non-linear Eqs. (29a)-(29c) with the help of the Newton-Raphson method. Further, the left superscripts t and t + Δ t indicate in which configuration at time t or time t + Δ t the quantity occurs [9]. Then, in accordance with this agreement we have

$$^{t+\Delta t}\overset{\circ}{\mathbf{E}} = {}^{t}\overset{\circ}{\mathbf{E}} + \Delta\overset{\circ}{\mathbf{E}}, \qquad ^{t+\Delta t}\overset{\wedge}{\mathbf{E}} = {}^{t}\overset{\wedge}{\mathbf{E}} + \Delta\overset{\wedge}{\mathbf{E}}, \tag{31a}$$

$$^{t+\Delta t}\overset{\circ}{\mathbf{H}} = {}^{t}\overset{\circ}{\mathbf{H}} + \Delta\overset{\circ}{\mathbf{H}}, \qquad ^{t+\Delta t}\overset{\wedge}{\mathbf{H}} = {}^{t}\overset{\wedge}{\mathbf{H}} + \Delta\overset{\wedge}{\mathbf{H}}, \tag{31b}$$

$$^{t+\Delta t}\mathbf{u} = {}^{t}\mathbf{u} + \Delta\mathbf{u}, \qquad ^{t+\Delta t}\mathfrak{I} = {}^{t}\mathfrak{I} + \Delta\mathfrak{I}, \tag{31c}$$

where $\Delta\overset{\circ}{\mathbf{E}}$, $\Delta\overset{\wedge}{\mathbf{E}}$, $\Delta\overset{\circ}{\mathbf{H}}$, $\Delta\overset{\wedge}{\mathbf{H}}$, $\Delta\mathbf{u}$ and $\Delta\mathfrak{I}$ are the incremental variables.

Substituting formulas (31a)-(31c) into Eqs. (29a)-(29c), and taking into account that the external loads and the second Piola-Kirchhoff stresses constitute the self-equilibrated system in the configuration at time t, one can obtain the following incremental equations:

$$\Delta\overset{\circ}{\mathbf{E}} = \left({}^{t}\overset{\circ}{\mathbf{M}} + \overset{\circ}{\mathbf{R}}\Delta\mathbf{u}\right)\Delta\mathbf{u}, \qquad \Delta\overset{\wedge}{\mathbf{E}} = \mathbf{Q}^{T}\left({}^{t}\overset{\wedge}{\mathbf{M}} + \overset{\wedge}{\mathbf{R}}\Delta\mathbf{u}\right)\Delta\mathbf{u}, \tag{32a}$$

$$\Delta\overset{\circ}{\mathbf{H}} = \mathbf{D}\Delta\overset{\circ}{\mathbf{E}}, \qquad \Delta\overset{\wedge}{\mathbf{H}} = \mathbf{Q}^{T}\mathbf{D}\mathbf{Q}\Delta\overset{\wedge}{\mathbf{E}}, \tag{32b}$$

$$2\left(\overset{\circ}{\mathbf{R}}\Delta\mathbf{u}\right)^{T}{}^{t}\overset{\circ}{\mathbf{H}} + \frac{2}{3}\left(\overset{\wedge}{\mathbf{R}}\Delta\mathbf{u}\right)^{T}\mathbf{Q}\,{}^{t}\overset{\wedge}{\mathbf{H}} + \left({}^{t}\overset{\circ}{\mathbf{M}} + 2\overset{\circ}{\mathbf{R}}\Delta\mathbf{u}\right)^{T}\Delta\overset{\circ}{\mathbf{H}} + \tag{32c}$$

$$+\frac{1}{3}\left({}^{t}\overset{\wedge}{\mathbf{M}} + 2\overset{\wedge}{\mathbf{R}}\Delta\mathbf{u}\right)^{T}\mathbf{Q}\Delta\overset{\wedge}{\mathbf{H}} = \Delta\mathfrak{I},$$

where ${}^{t}\overset{\circ}{\mathbf{M}}$ and ${}^{t}\overset{\wedge}{\mathbf{M}}$ are the matrices of order 5×8, corresponding to the configuration at time t:

$${}^{t}\overset{\circ}{\mathbf{M}} = \overset{\circ}{\mathbf{B}} + 2\overset{\circ}{\mathbf{R}}{}^{t}\mathbf{u}, \qquad {}^{t}\overset{\wedge}{\mathbf{M}} = \overset{\wedge}{\mathbf{B}} + 2\overset{\wedge}{\mathbf{R}}{}^{t}\mathbf{u}.$$

Eliminating incremental strains and incremental stress resultants from Eqs. (32a)-(32c) and introducing the matrix

$$\overset{\wedge}{\mathbf{D}} = \mathbf{Q}\mathbf{Q}^{T}\mathbf{D}\mathbf{Q}\mathbf{Q}^{T},$$

one obtains the governing incremental equilibrium equations

$$\mathbf{G}(\Delta\mathbf{u}) = 2\left(\overset{\circ}{\mathbf{R}}\,\Delta\mathbf{u}\right)^{\mathrm{T}}\,{}^{t}\overset{\circ}{\mathbf{H}} + \frac{2}{3}\left(\hat{\mathbf{R}}\,\Delta\mathbf{u}\right)^{\mathrm{T}}\mathbf{Q}\,{}^{t}\hat{\mathbf{H}} + \left({}^{t}\overset{\circ}{\mathbf{M}} + 2\overset{\circ}{\mathbf{R}}\,\Delta\mathbf{u}\right)^{\mathrm{T}}\mathbf{D}\left({}^{t}\overset{\circ}{\mathbf{M}} + \overset{\circ}{\mathbf{R}}\,\Delta\mathbf{u}\right)\Delta\mathbf{u} + \quad (33)$$

$$+\frac{1}{3}\left({}^{t}\hat{\mathbf{M}} + 2\hat{\mathbf{R}}\,\Delta\mathbf{u}\right)^{\mathrm{T}}\hat{\mathbf{D}}\left({}^{t}\hat{\mathbf{M}} + \hat{\mathbf{R}}\,\Delta\mathbf{u}\right)\Delta\mathbf{u} = \Delta\mathfrak{I}.$$

Due to the existence of the non-linear terms in Eq. (33), the Newton-Raphson iteration process should be employed to solve these equations

$$\Delta\mathbf{u}^{[n+1]} = \Delta\mathbf{u}^{[n]} + \left[\frac{\partial\mathbf{G}}{\partial\Delta\mathbf{u}}\left(\Delta\mathbf{u}^{[n]}\right)\right]^{-1}\left[\Delta\mathfrak{I} - \mathbf{G}\left(\Delta\mathbf{u}^{[n]}\right)\right], \quad (34)$$

where $n = 0, 1, \ldots$.

The equilibrium equations (34) for each element are assembled by the usual techniques to form the global incremental equilibrium equations. These incremental equations should be performed until the required accuracy of the solution can be obtained. The convergence criterion used herein can be described as

$$\left\|\Delta\mathbf{U}^{[n+1]} - \Delta\mathbf{U}^{[n]}\right\| < \varepsilon\left\|\Delta\mathbf{U}^{[n]}\right\|, \quad (35)$$

where $\|\bullet\|$ stands for the Euclidean norm in the displacement space; $\Delta\mathbf{U}$ is the global vector of displacement increments; ε is the priori chosen tolerance.

6 Numerical results

Three tests were employed to assess the effectiveness of this element. They are a cantilever beam subjected to a conservative transverse load at the tip, and isotropic and composite cantilever beams subjected to non-conservative couple forces at the tip. In all tests the tolerance error ε from relation (35) is set to be $\varepsilon = 10^{-6}$.

6.1. Cantilever beam under conservative load

This problem has been extensively treated for numerical testing of non-linear finite element models (see, for example Refs. [8] and [13]). The cantilever beam has a rectangular cross section, and its mechanical and geometrical characteristics are given in Fig. 4.

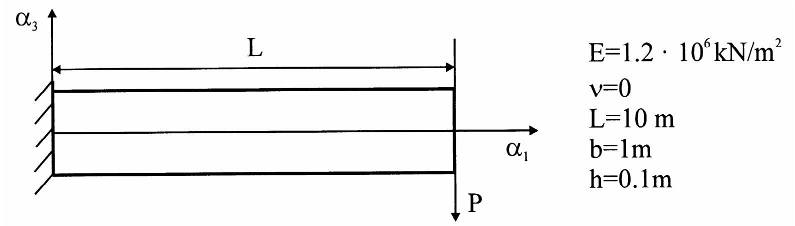

Fig. 4 Cantilever beam under conservative load

Fig. 5 presents the dependence of the tip displacements of the middle line $v_i = \left(v_i^- + v_i^+\right)/\,2$ on the conservative load P. The solid lines correspond to the present element while the dashed lines correspond to the finite element based on the strain-displacement relationships (8) without the thickness change, i.e., $v_3^- = v_3^+ = v_3$. As

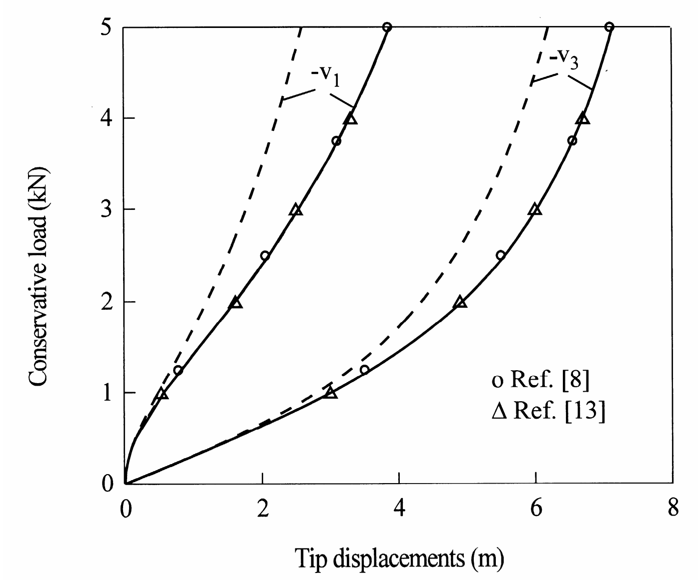

Fig. 5 Longitudinal and transverse tip displacements of cantilever beam under conservative load

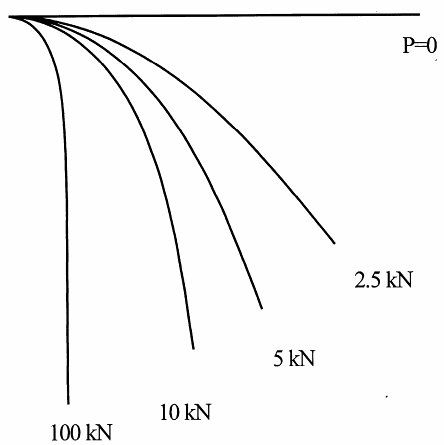

Fig. 6 Deformed configurations of cantilever beam under conservative load

can be seen in Fig. 5, using these relationships, which are not free for large rigid body motions, without special stabilization algorithms leads to an incorrect description of the deformed configuration of the beam undergoing large rotations. The results marked by ○ and Δ were obtained in Refs. [8] and [13] by using 4 loading steps in increments of 1.25 kN and 1.0 kN, respectively. One can observe that all elements perform well. It should be mentioned that we use only one loading step to obtain all results represented in Fig. 5. Moreover, we need only one loading step to obtain the results by increasing a load to 100 kN and more. In this problem we did not discover an escape of the initial value from Newton's attraction area for all reasonable levels of loading. The deformed configurations of the beam for various conservative concentrated loads are displayed in Fig. 6.

Additionally, Table lists the convergence results. It is seen that 5 or 10 elements are quite enough to obtain the good accuracy for engineering calculations. The converged solution is achieved with 17-19 iterations for P=100 kN and their number depends on the number of elements. It is interesting to note that, when we used 2 or 10 incremental loading steps to determine a beam response for P=100 kN, the results were exactly the same but the final number of iterations was more.

6.2. Isotropic cantilever beam under non-conservative couple forces

The isotropic cantilever beam subjected to couple forces at the tip (Fig. 7) was selected to study the effect of non-conservative loading. Non-conservative loading is simulated by a pair of opposite forces whose directions are always perpendicular to the

Table

Tip displacements of cantilever beam under conservative load

Elements	P = 5 kN		P = 10 kN		P = 100 kN	
	$-v_1$	$-v_3$	$-v_1$	$-v_3$	$-v_1$	$-v_3$
5	3.930	7.197	5.664	8.188	8.861	9.523
10	3.890	7.153	5.578	8.128	8.688	9.477
20	3.881	7.142	5.558	8.113	8.615	9.440
40	3.878	7.140	5.553	8.109	8.597	9.429
80	3.878	7.139	5.552	8.108	8.593	9.426

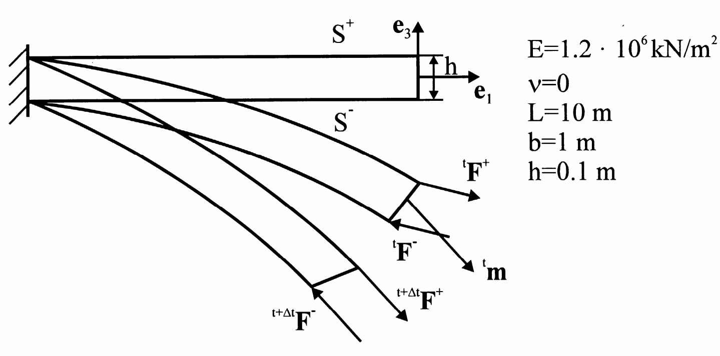

Fig. 7 Deformed configurations of cantilever beam under non-conservative forces

current end cross section. During calculations the loading increments are taken to be equal and small in each loading step, to bend a beam into a closed circle. For this purpose the following expressions for the applied incremental forces should be used:

$$\Delta\mathbf{F}^{\pm} = {}^{t+\Delta t}\mathbf{F}^{\pm} - {}^{t}\mathbf{F}^{\pm}, \tag{36}$$

$${}^{t}\mathbf{F}^{\pm} = \pm {}^{t}P\, {}^{t-\Delta t}\mathbf{m}, \qquad {}^{t+\Delta t}\mathbf{F}^{\pm} = \pm\left({}^{t}P + \Delta P\right){}^{t}\mathbf{m},$$

$${}^{t}\mathbf{m} = \frac{1}{\sqrt{1+2\,{}^{t}E_{33}}}\left[\left(1+{}^{t}\beta_3\right)\mathbf{e}_1 - {}^{t}\beta_1\mathbf{e}_3\right], \qquad {}^{t}E_{33} = {}^{t}\beta_3 + \frac{1}{2}\left({}^{t}\beta_1\right)^2 + \frac{1}{2}\left({}^{t}\beta_3\right)^2,$$

where ${}^{t}P$ is the loading parameter in the current configuration at time t; ${}^{t}\mathbf{m}$ is the unit vector normal to the end cross section in the current configuration at time t (Fig. 7); ΔP is the loading increment.

The beam is discretized by 20 present two-node elements. The load is applied in 196 steps of equal magnitude $\Delta P = \pi$ kN . In a result the following accuracy was achieved

$$\left|1 + v_1 / L\right| < 10^{-3} \quad \text{and} \quad \left|v_3 / L\right| < 10^{-3}. \tag{37}$$

The results of the solution of this problem are shown in Figs. 8 and 9. Fig. 9 shows that deformed configurations are circular arcs as predicted by the elasticity theory. An agreement with the analytical solution is good since an exact value of the bending moment at the tip is $M^e = 20\pi$. Our finite element solution gives $P = 196\pi$, i.e., the applied moment at the tip will be $M = Ph = 19{,}6\pi$. The better accuracy one can achieve if more increments will be used.

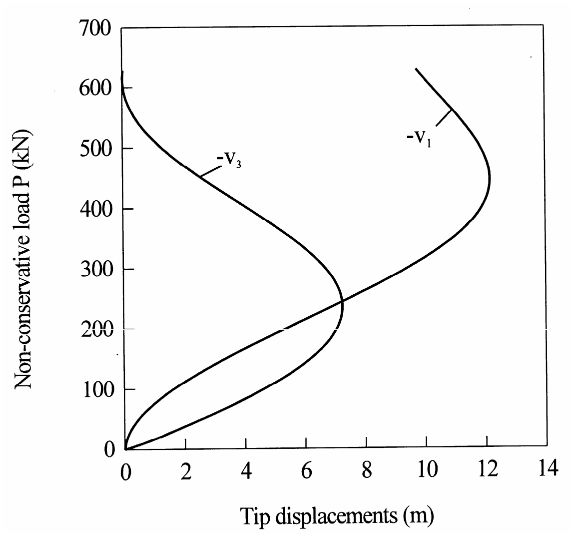

Fig. 8 Longitudinal and transverse tip displacements of isotropic cantilever beam under non-conservative couple forces

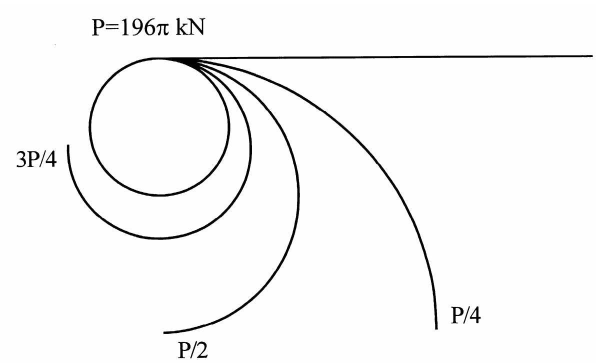

Fig. 9 Deformed configurations of isotropic cantilever beam under non-conservative couple forces

6.3. Two-layered composite cantilever beam under non-conservative couple forces

The two-layered composite cantilever beam subjected to couple forces at the tip (Fig. 10) was selected to investigate the influence of the laminated material response and non-conservative loading on non-linear beam behaviour. The geometrical and material characteristics of a beam are shown in Fig. 10, where L and T refer to the longitudinal and transverse directions of the individual ply. Herein we consider the similar problem of bending a straight beam into a perfect circle (see the previous section). The non-conservative loads are computed accordingly to Eq. (36). The beam is also discretized by 20 two-node elements but the load is applied in 501 steps of equal magnitude

$\Delta P = 0{,}2$ kN , to obtain the required accuracy (37). The results of our finite element formulation are presented in Figs. 11 and 12.

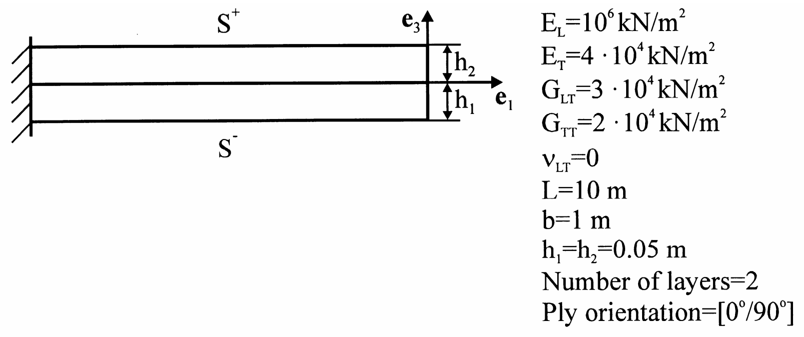

Fig. 10 Two-layered composite cantilever beam under non-conservative couple forces

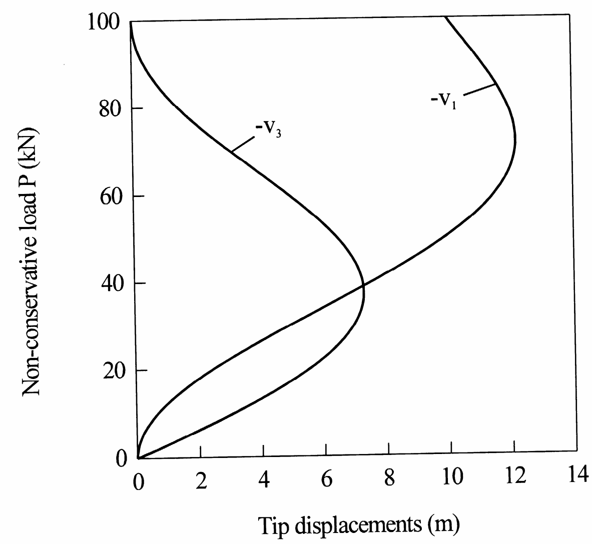

Fig. 11 Longitudinal and transverse tip displacements of two-layered composite cantilever beam under non-conservative couple forces

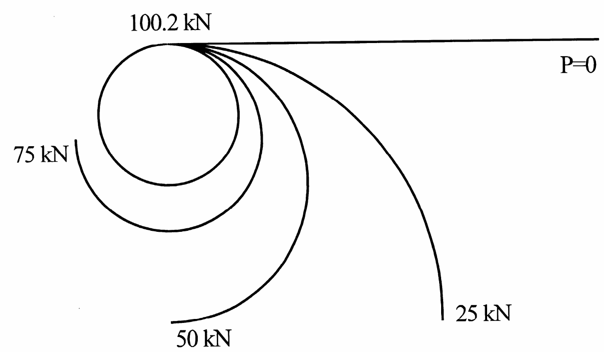

Fig. 12 Deformed configurations of two-layered composite cantilever beam under non-conservative couple forces

7 Conclusions

The simple and efficient mixed finite element model has been developed for the analysis of multilayered composite Timoshenko beams undergoing finite rotations. The finite element formulation is based on the non-linear strain-displacement equations that are completely free for arbitrarily large rigid body motions. As fundamental unknowns four displacements and five strains of the face lines, and also five stress resultants have been chosen.

The simplest two-node beam element and assumed strain concept have been used without special stabilization algorithms. The element characteristics arrays have been obtained by applying the Hu-Washizu mixed variational principle in conjunction with the total Lagrangian formulation and Newton-Raphson method. The elemental matrices require only direct substitutions (no inversion is needed) and they have been evaluated using the full exact analytical integration. Therefore, our finite element formulation is very simple and economical and our element does not contain any spurious zero energy modes.

To demonstrate the high accuracy and effectiveness of the developed non-linear finite element model, three tests for the cantilever beams under conservative and non-conservative loading were employed. It has been shown that for a case of conservative loading only one loading step is needed to obtain the computationally exact solution of the beam problems for very high level of loading.

The extension to the layer-wise Timoshenko beam theory [19] undergoing finite rotations poses no additional difficulties but requires algebra and computation efforts. This problem is currently under development and will be presented in the next paper.

References

1. G. Cantin. Strain displacement relationships for cylindrical shells, AIAA Journal 6 (1968) 1787-1788.
2. D.J. Dawe. Rigid-body motions and strain-displacement equations of curved shell finite elements, International Journal of Mechanical Sciences 14 (1972) 569-578.
3. G.M. Kulikov and S.V. Plotnikova. Simple and effective elements based upon Timoshenko-Mindlin shell theory, Computer Methods in Applied Mechanics and Engineering (2002) (in press).
4. G.M. Kulikov and S.V. Plotnikova. Efficient mixed Timoshenko-Mindlin shell elements, International Journal for Numerical Methods in Engineering (2002) (in press).
5. G.M. Kulikov and S.V. Plotnikova. Comparative analysis of two algorithms for numerical solution of nonlinear static problems for multilayered anisotropic shells of revolution, 2. Account of transverse compression, Mechanics of Composite Materials 35 (1999) 293-300.
6. G.M. Kulikov. Refined global approximation theory of multilayered plates and shells, Journal of Engineering Mechanics 127 (2001) 119-125.
7. G.M. Kulikov. Analysis of initially stressed multilayered shells, International Journal of Solids and Structures 38 (2001) 4535-4555.
8. A. Barut, E. Madenci and A. Tessler. Nonlinear analysis of laminates through a Mindlin-type shear deformable shallow shell element, Computer Methods in Applied Mechanics and Engineering 143 (1997) 155-173.
9. K.J. Bathe. Finite Element Procedures (Prentice Hall, NJ, 1996).
10. P. Betsch and E. Stein. An assumed strain approach avoiding artificial thickness straining for a nonlinear 4-node shell element, Communications in Numerical Methods in Engineering 11 (1995) 899-909.
11. N. Büchter and E. Ramm. Shell theory versus degeneration - a comparison in large rotation finite element analysis, International Journal for Numerical Methods in Engineering 34 (1992) 39-59.
12. T.J.R. Hughes and E. Carnoy. Non-linear finite element shell formulation accounting for large membrane strains, Computer Methods in Applied Mechanics and Engineering 39 (1983) 69-82.

13. G. Horrigmoe and P.G. Bergan. Nonlinear analysis of free-form shells by flat finite elements, Computer Methods in Applied Mechanics and Engineering 16 (1978) 11-35.

14. I. Kreja, R. Schmidt and J.N. Reddy. Finite elements based on a first-order shear deformation moderate rotation shell theory with applications to the analysis of composite structures, International Journal of Non-Linear Mechanics 32 (1997) 1123-1142.

15. M. Li. The finite deformation theory for beam, plate and shell. Part I. The two-dimensional beam theory, Computer Methods in Applied Mechanics and Engineering 146 (1997) 53-63.

16. J.C. Simo, D.D. Fox and M.S. Rifai. On a stress resultant geometrically exact shell model. Part III: Computational aspects of the nonlinear theory, Computer Methods in Applied Mechanics and Engineering 79 (1990) 21-70.

17. T.J.R. Hughes and T.E. Tezduyar. Finite elements based upon Mindlin plate theory with particular reference to the four-node bilinear isoparametric element, Journal of Applied Mechanics 48 (1981) 587-596.

18. S.P. Timoshenko. On the correction for shear of the differential equation for transverse vibrations of prismatic bars, Philosophical Magazine and Journal of Science Ser. 6, 41 (245) (1921) 744-746.

19. E.I. Grigolyuk and G.M. Kulikov. Multilayered Reinforced Shells: Analysis of Pneumatic Tires (Mashinostroyenie, Moscow, 1988) (in Russian).

20. K. Washizu. Variational Methods in Elasticity and Plasticity (Pergamon Press, Oxford, 1982).

Расчет прямолинейных композитных балок при больших поворотах методом конечных элементов

Г.М. Куликов, С.В. Плотникова

Кафедра "Прикладная математика и механика", ТГТУ

Ключевые слова и фразы: конечные повороты; теория балок Тимошенко; большие перемещения твердого тела.

Аннотация: Для расчета многослойных композитных балок при больших поворотах разработана простая и эффективная модель балки Тимошенко на основе использования смешанных конечноэлементных аппроксимаций, а также инкрементального подхода в полной Лагранжевой формулировке в сочетании с методом Ньютона-Рафсона. При этом учтены деформации поперечного сдвига и поперечные нормальные деформации. Предложены новые деформационные соотношения, которые точно представляют большие перемещения балочного элемента как твердого целого. В качестве искомых функций выбраны 4 перемещения и 5 деформаций лицевых плоскостей балки, а также 5 результирующих напряжений. Разрешающие уравнения МКЭ получены путем использования смешанного вариационного принципа Ху-Васидзу. Приведены результаты численных расчетов, подтверждающих эффективность разработанного подхода.

Berechnung der geradelinigen Kompositbalken bei den großen Drehungen durch die Methode der endlichen Elemente

Zusammenfassung: Für die Berechnung der vielschichtigen Kompositbalken bei den großen Drehungen ist ein einfaches und effektives Modell des Timoschenko-Balkens auf Grund der Benutzung von gemischten endlichelementlichen Approksimationen als auch des Inkrementalherangehens in der vollen Lagrangenformulierung im

Zusammenhang mit der Njuton-Rafson-Methode erarbeitet. Dabei sind die Deformierungen des Blattes und quere Normalumformungen berücksichtigt. Es sind neue Deformationsverhältnisse vorgeschlagen, die die große Umstellungen des Balkenelementes als harte Ganzheit darstellen. Als gesuchte Funktionen sind 4 Umstellungen und 5 Umformungen der Gesichtsflächen des Balkens und auch 5 resultierenden Spannungen ausgewählt. Die Gleichungen sind durch die Benutzung des gemischten variierenden Hu-Wasidzu-Prinzipes erhalten. Es sind Resultate der Zahlberechnungen angeführt, die die Effektivität des erarbeiteten Herangehens bestätigen.

Calcul des poutres composites rectilignes avec de grands tournants par la méthode des éléments finis

Résumé: Pour le calcul des poutres multicouches rectilignes avec de grands tournants est élaboré un modèle efficace de la poutre qui porte le nom de Timochenko à la base de l'utilisation des approximations mixtes des éléments finis, ainsi que l'approche incrémentale dans la formulation complète de Lagrange en combinaison avec la méthode de Newton-Raphson. Avec cela sont mises en compte les déformations du décalage transversale et les déformations transversales normales. Sont proposées de nouvelles relations de déformations qui représentent précisement les grands déplacements de l'élément de poutre comme un ensemble solide. En qualité de fonctions recherchées sont choisies quatre déplacements et cinq déformations des surfaces de la poutre ainsi que cinq tensions résultantes. Des équations permettantes sont obtenues par l'utilisation du principe mixte de variation Hu-Washizu. Sont cités les résultats des calculs numériques, confirmant l'efficacité de l'approche élaborée.
